Conformational Transitions of Subunit ε in ATP Synthase from Thermophilic *Bacillus* PS3

Boris A. Feniouk,[†] Yasuyuki Kato-Yamada,[‡] Masasuke Yoshida,[†§*] and Toshiharu Suzuki[†]
[†]ICORP ATP Synthesis Regulation Project, Japan Science and Technology Corporation, Tokyo, Japan; [‡]College of Science, Rikkyo (St. Paul's) University, Tokyo, Japan; and [§]Faculty of Engineering, Kyoto Sangyo University, Kyoto, Japan

ABSTRACT Subunit ε of bacterial and chloroplast F_OF_1-ATP synthase is responsible for inhibition of ATPase activity. In *Bacillus* PS3 enzyme, subunit ε can adopt two conformations. In the "extended", inhibitory conformation, its two C-terminal α-helices are stretched along subunit γ. In the "contracted", noninhibitory conformation, these helices form a hairpin. The transition of subunit ε from an extended to a contracted state was studied in ATP synthase incorporated in *Bacillus* PS3 membranes at 59°C. Fluorescence energy resonance transfer between fluorophores introduced in the C-terminus of subunit ε and in the N-terminus of subunit γ was used to follow the conformational transition in real time. It was found that ATP induced the conformational transition from the extended to the contracted state (half-maximum transition extent at 140 μM ATP). ADP could neither prevent nor reverse the ATP-induced conformational change, but it did slow it down. Acid residues in the DELSEED region of subunit β were found to stabilize the extended conformation of ε. Binding of ATP directly to ε was not essential for the ATP-induced conformational change. The ATP concentration necessary for the half-maximal transition (140 μM) suggests that subunit ε probably adopts the extended state and strongly inhibits ATP hydrolysis only when the intracellular ATP level drops significantly below the normal value.

INTRODUCTION

H^+-F_OF_1-ATP synthase is found in bacterial plasma membranes, thylakoid membranes of chloroplasts, and inner mitochondrial membranes (1,2). The enzyme uses the energy of the transmembrane electrochemical proton potential difference ($\Delta\tilde{\mu}_{H^+}$) to synthesize ATP from ADP and P_i. The simplest forms of bacterial F_OF_1, including *Bacillus* PS3 enzyme, have eight types of subunits. Five subunits (in stoichiometry $\alpha_3\beta_3\gamma_1\delta_1\varepsilon_1$) comprise hydrophilic F_1, which bears nucleotide-binding sites. Three subunits (in stoichiometry $a_1b_2c_{10}$) comprise membrane-embedded F_O, which is responsible for proton translocation. Three $\alpha\beta$ pairs form a hexamer, and elongated subunit γ fills its central cavity (3–5). Subunits c form a ring-shaped oligomer (6–8) that binds to the $\gamma\varepsilon$-complex (6,9).

During catalysis, proton translocation powers the rotation of the c-oligomer (and the $\gamma\varepsilon$-complex bound to it) relative to the $ab_2\alpha_3\beta_3\delta_1$-complex (10–13). Rotation of the $\gamma\varepsilon$-complex inside the $\alpha_3\beta_3$-hexamer induces cyclic conformational changes in catalytic sites that result in substrate binding and product release (14–17).

When the $\Delta\tilde{\mu}_{H^+}$ is low, the enzyme operates as an ATP-driven proton pump. This activity reversal can be important for such functions as maintaining the $\Delta\tilde{\mu}_{H^+}$ necessary for ion transport and flagella motility in bacteria or pumping out H^+ in acidophiles. However, uncontrolled ATPase activity can quickly exhaust the intracellular ATP pool. Several regulatory features prevent this by selectively inhibiting ATP hydrolysis, but not synthesis (2), converting the protein from a mere catalyst that speeds up both forward and reverse reactions into a unidirectional molecular machine.

One such feature found in bacterial and chloroplast F_OF_1-ATP synthase is the inhibition of ATPase activity by subunit ε (18–20). Subunit ε is a small, 15 kDa protein consisting of two domains: the N-terminal β-sandwich and the C-terminal pair of α-helices. Only the latter domain is responsible for the inhibition (21–28). Numerous studies have revealed that subunit ε can undergo large conformational changes (25,29–35). Some details of these conformational changes were elucidated by x-ray and NMR studies demonstrating that the C-terminal domain of ε can adopt at least two conformations: a hairpin-like contracted state (the "down state"; Fig. 1 *B*, state *III*) (6,33,36–38) and an extended state with the two α-helices stretched along subunit γ toward the $\alpha_3\beta_3$-hexagon (the "up state"; Fig. 1 *B*, state *I*) (39,40). In later studies, these two different states were trapped by cross-linking in F_OF_1 from *Escherichia coli* (41) and *Bacillus* PS3 (42). It was also found that fixing subunit ε in the contracted hairpin-like state abolishes the inhibitory effect (41,42).

Experiments on *Bacillus* PS3 enzyme have been particularly fruitful in elucidating the inhibitory function of subunit ε. It was found that in the presence of ATP, subunit ε adopts a noninhibitory contracted conformation, whereas in the presence of ADP, the inhibitory extended state is observed. As a possible explanation, it was suggested that the ATP/ADP ratio determines the conformation of subunit ε (42).

It was also suggested that electrostatic interactions between the positively charged residues in the C-terminal domain of ε and the negatively charged residues in the

Submitted August 5, 2009, and accepted for publication October 15, 2009.

*Correspondence: myoshida@res.titech.ac.jp

Editor: Robert Nakamoto.

0006-3495/10/02/0434/9 $2.00

doi: 10.1016/j.bpj.2009.10.023

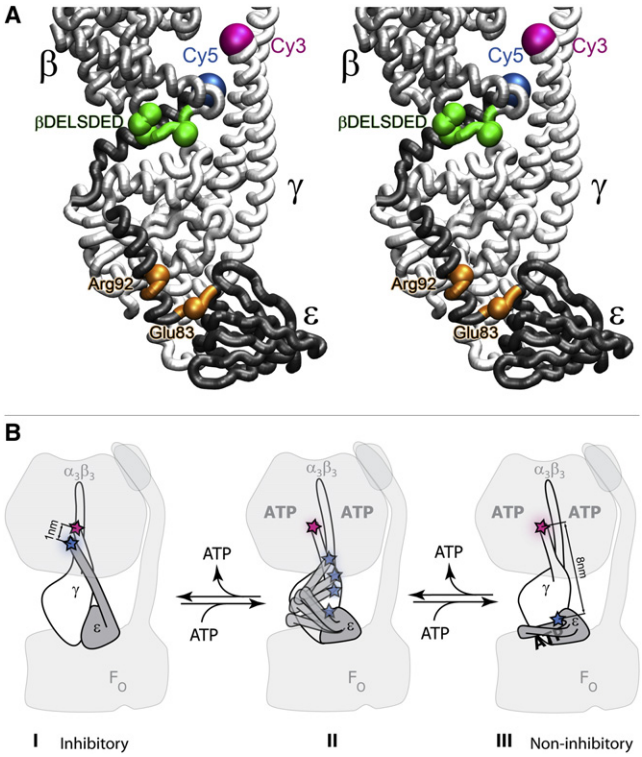

FIGURE 1 (*A*) Stereo cartoon representation of subunit ε (*dark gray*) in an extended conformation. Partly shown are subunit γ (*white*) and subunit β proximal to the C-terminal domain of ε. Fluorescent labels are shown as large colored spheres (*magenta*: Cy3 on the N-terminus of γ; *blue*: Cy5 on the C-terminus of ε). Residues mutated to reduce the affinity of subunit ε to ATP are shown as small orange spheres, and the βDELSDED region is shown in green. The figure was generated from Protein Data Bank entry 1JNV of the *E. coli* $\alpha_3\beta_3\gamma\varepsilon$ complex (40) with VMD software (53). (*B*) Cartoon scheme of subunit ε conformational transitions in *Bacillus* PS3 F_OF_1 ATP synthase. Subunit γ is shown in white, subunit ε in dark gray, and $\alpha_3\beta_3\delta$-complex and F_O in light gray. Positions of introduced Cy3 on subunit γ and Cy5 on subunit ε are indicated by a magenta and blue star, respectively. See details at the end of the Discussion.

DELSDED region of subunit β (*green* in Fig. 1 *A*) are involved in propagating the inhibitory effect of subunit ε (43). However, it remained unclear whether the electrostatic interactions with βDELSDED play any role in the conformational changes of ε.

A peculiar feature of *Bacillus* PS3 F_OF_1 is that ATP can bind directly to subunit ε (44,45). The recently published structure of the ε-ATP complex confirms that ATP binds when subunit ε is in the hairpin noninhibitory conformation (46). Mutagenesis experiments revealed that weaker binding of ATP to isolated subunit ε correlated with greater inhibition of $\alpha_3\beta_3\gamma\varepsilon$-complex ATPase activity, suggesting a regulatory role for ATP binding to ε in vivo (47).

To our knowledge, the detailed mechanism and kinetics of subunit ε conformational transitions in the whole F_OF_1 from *Bacillus* PS3 have not yet been studied. However, some results have been obtained on the isolated F_1 portion. Iino et al. (48) used specific labeling by fluorophores at the C-terminus of subunit ε and the N-terminus of subunit γ (Cy5 and Cy3, respectively; see Fig. 1) to monitor the conformational transitions in real time by measuring the fluorescence energy resonance transfer (FRET) from Cy3 to Cy5. They confirmed that ATP induces the transition of ε into the contracted state. They also found that when ATP was hydrolyzed to ADP by hexokinase, the reverse conformational change to the extended state of subunit ε occurred, in line with the suggested role of the ATP/ADP ratio. However, it remained ambiguous whether ADP exerts any direct effect on subunit ε, or whether it is the absence of ATP that matters. It was also unclear how the binding of ATP to subunit ε influences its conformational transitions.

We applied the FRET technique described above to investigate the conformational transitions of subunit ε in whole *Bacillus* PS3 F_OF_1 in native uncoupled membranes at 59°C in the presence of both ATP and ADP.

MATERIALS AND METHODS

Expression and purification of F_1

Escherichia coli cells expressing *Bacillus* PS3 F_OF_1 (His-tagged at β-subunits, lacking subunit ε and with a cysteine introduced in position 3 of subunit γ, named $\gamma_{Cys}F_1$-$\Delta\varepsilon$) were grown and collected as described previously (42,49). DK8 *E. coli* cells (bglR, thi-1, rel-1, HfrPO1, Δ(*unc*B-*uncC*), ilv:Tn10) lacking the wild-type (WT) F_OF_1 operon were used for expression. The $\gamma_{Cys}F_1$-$\Delta\varepsilon$ complex was purified by Ni-NTA affinity chromatography as described in the Supporting Material.

Bacillus PS3 ATP synthase subunit ε with a cysteine introduced in position 134 (ε_{Cys}) was expressed and purified as described previously (44,48). Mutant εEARA subunit ε was engineered from ε_{Cys} by substitution of residues εGlu-83 and εArg-92 to alanines as described by Kato-Yamada and Yoshida (44).

Labeling of subunits γ

The purified $F_1\Delta\varepsilon$ with mutation S3C in subunit γ ($\gamma_{Cys}F_1$-$\Delta\varepsilon$) was treated for 1 h with 2 mM dithiothreitol (DTT) at 42°C. The sample was then passed through a NAP-10 gel filtration column equilibrated with buffer containing 100 mM KCl, 20 mM K_2HPO_4, 2.5 mM EDTA, pH 6.6. Then the sample was diluted to 4 mg/mL protein by the same buffer, and Cy3-maleimide was added to a final concentration of 100 μM from 5 mM stock solution in *N*,*N*-dimethyl formamide. After a 2 h incubation in darkness at room temperature, the reaction was stopped by addition of DTT to 2 mM.

Reconstitution of $F_1\Delta\varepsilon$ with subunit ε

E. coli cells expressing *Bacillus* PS3 ε_{Cys} (4 g, wet weight) were suspended in 70 mL of buffer containing 10% glycerol, 20 mM HEPES-KOH (pH 7.5), and 2.5 mM $MgCl_2$, passed twice through a French press, and mixed with 3 mL of $F_1\Delta\varepsilon$ labeled by Cy3-maleimide. The mixture was heated to 57°C for 10 min, and centrifuged at 190,000 × *g* at 4°C for 1 h. The supernatant was applied to a NiNTA column, and reconstituted F_1 (with Cy3-labeled subunit γ and unlabeled subunit ε) was purified as described above. The purified protein was labeled by Cy5-maleimide according to the Cy3-maleimide labeling protocol.

The resulting F_1 labeled by Cy3 at γCys3, and by Cy5 at εCys-134 was concentrated as described above, and the excess Cy5 was removed on a NAP-10 column equilibrated with buffer containing 10% glycerol, 20 mM HEPES-KOH (pH 7.5), and 2.5 mM $MgCl_2$. The labeling efficiency

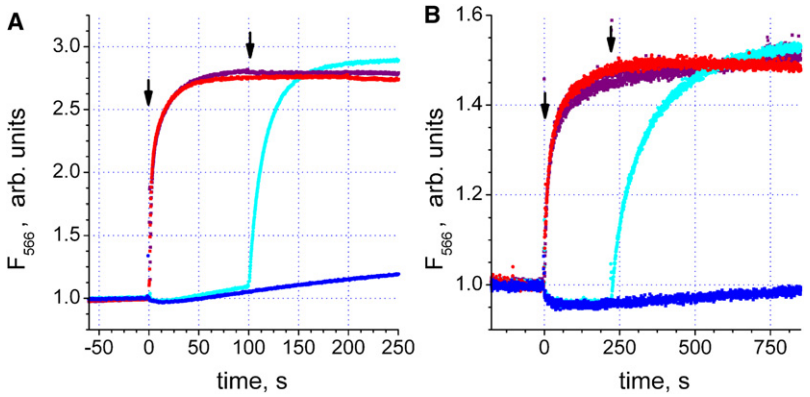

FIGURE 2 Effect of ATP and ADP on the conformational state of subunit ε, as monitored via fluorescence of Cy3 at 566 nm. Measurements were done at 59°C in buffer containing 100 mM KCl, 1 mM $MgCl_2$, 20 mM MES, 20 mM MOPS, 20 mM HEPES, 20 mM Tricine, 10% v/v glycerol, pH 7.9. Arrows indicate addition of nucleotides. Note the different timescales in panels *A* and *B*. Red traces: ATP added to 250 μM at time 0, no other additions. Purple traces: ATP added to 250 μM at time 0, ADP added later to 1 mM. Blue traces: ADP added to 1 mM at time 0, no other additions. Cyan traces: ADP added to 1 mM at time 0, ATP added later to 250 μM. (*A*) isolated F_1. (*B*) F_1 reconstituted with *Bacillus* PS3 inverted EDTA-treated membranes.

was checked by means of the absorption spectrum as described previously (48) and was found to be 50–60% for subunit γ and 95% for subunit ε.

After purification was completed, the protein was concentrated to 2 mg/mL and stored at −80°C.

Reconstitution of F_1 into EDTA-treated membranes

Inverted *Bacillus* PS3 membrane vesicles stripped of F_1 were prepared by sonication of *Bacillus* PS3 cells in buffer containing 2 mM EDTA and 2 mM sodium succinate (see the Supporting Material for details). Residual ATPase activity was inhibited by 7-chloro-4-nitrobenzo-2-oxa-1,3-diazole (NBD-Cl) treatment as described previously (50). For reconstitution, stripped membranes were mixed with an excess of purified F_1, heated for 5 min to 60°C, and incubated for 30 min at room temperature. The excess F_1 was washed away by the same buffer in two sequential centrifugations (190,000 × *g*, 45 min, 4°C). The reconstituted membranes were frozen in liquid nitrogen and stored at −80°C until they were used.

FRET measurements

FRET from Cy3 on subunit γ to Cy5 on subunit ε was monitored via Cy3 fluorescence on an FP-6500 fluorometer (Jasco, Tokyo, Japan) as described previously (48), with minor modifications (see the Supporting Material). Measurements were obtained in buffer containing 100 mM KCl, 1 mM $MgCl_2$, 20 mM MES, 20 mM MOPS, 20 mM HEPES, 20 mM Tricine, 10% v/v glycerol, pH 7.9. The F_1 concentration in the cuvette was 3–10 μg/mL. In the case of reconstituted membranes, the total protein concentration was 20–60 μg/mL, corresponding to F_1 concentrations in the range of 0.6–3.5 μg/mL, as estimated by the initial fluorescence level. All FRET measurements were done at 59°C.

Measurement of ATPase activity

ATPase activity was measured via Phenol Red absorption changes as described previously (51), with minor modifications. See details in the Supporting Material.

RESULTS

ADP cannot reverse the ATP-induced conformational transition of ε

In previous studies of *Bacillus* PS3 enzyme, it was determined that 1), ATP induces the conformational transition of subunit ε from an extended to a contracted state; and 2), if all ATP is hydrolyzed to ADP, a reverse transition to an extended conformation occurs (42,48). However, it was unclear which factor (i.e., the ATP/ADP ratio or just the ATP concentration) determines the conformation of ε. To clarify this issue, we investigated the effects of ATP and ADP in isolated F_1 and in F_OF_1 in inverted *Bacillus* PS3 membranes.

As can be seen in Fig. 2, the addition of ATP to 250 μM caused a marked increase in the Cy3 fluorescence both in isolated F_1 and in F_OF_1 incorporated in *Bacillus* PS3 inverted membranes (*red trace*). It should be noted that the addition of MgATP complex was necessary to induce the transition. As documented in Fig. S6, Mg-free ATP (as well as Mg^{2+} without ATP) induced no significant changes in Cy3 fluorescence.

When ADP alone was added to the sample to 1 mM (*blue* and *cyan traces*), no major change in the Cy3 fluorescence occurred. The slow, minor rise in the fluorescence observed after ADP addition was due to contaminating ATP in the commercial ADP used; this rise could be significantly decreased by the addition of a glucose-hexokinase trap (not documented).

When ADP was added to 1 mM after 250 μM ATP (*purple traces*), no significant fluorescence decrease was observed. This result demonstrates that ADP failed to cause a reverse transition of ε from the ATP-induced contracted state.

The presence of 1 mM ADP also did not prevent subunit ε transition induced by 250 μM ATP (compare *cyan* and *red traces* in Fig. 2). The extent of the fluorescence change was not diminished in the presence of ADP. The effects described were observed both for isolated F_1 (Fig. 2 *A*) and for F_OF_1 in *Bacillus* PS3 membranes (Fig. 2 *B*). The results imply that a >400-fold change in the ATP/ADP ratio had no major effect on the final conformation of subunit ε.

However, ADP lowered the rate of ATP-induced transition. The half-rise time for the fluorescence change increased from ≈3 s (no ADP) to ≈9 s (1 mM ADP) in isolated F_1, whereas in F_OF_1 the half-rise time increased from ≈15 to ≈74 s (Fig. 2).

How much ATP is needed to induce the conformational transition of ε in F_1 and F_OF_1?

As documented in Fig. 2, the addition of ATP caused an increase in Cy3 fluorescence in both isolated F_1 and the whole F_OF_1. The extent of this increase was dependent on the final concentration of ATP added (Fig. 3). The dependence was different for isolated F_1 and the whole F_OF_1 in uncoupled membrane. The apparent K_d for ATP was 30 ± 2 μM in isolated F_1, but it increased to 141 ± 8 μM after reconstitution of F_1 with EDTA-treated *Bacillus* PS3 inverted membranes (Fig. 3). The Hill numbers, however, were similar: 1.60 ± 0.14 in isolated F_1 and 1.76 ± 0.13 in the whole F_OF_1.

In full agreement with previous results (48), in isolated F_1 the kinetics of ATP-induced Cy3 fluorescence increase was apparently biexponential. The same was true for the whole F_OF_1 (Table 1; see also Fig. S2). Of note, the relative input of the faster and slower apparent components (≈60% and ≈40%, respectively) was the same for isolated F_1 and the whole F_OF_1 within experimental error.

However, the time constant of each kinetic component was larger in the case of the whole F_OF_1. The results in Table 1 indicate that binding of F_1 to F_O slowed down the conformational transition of ε induced by 1 mM ATP ~6-fold.

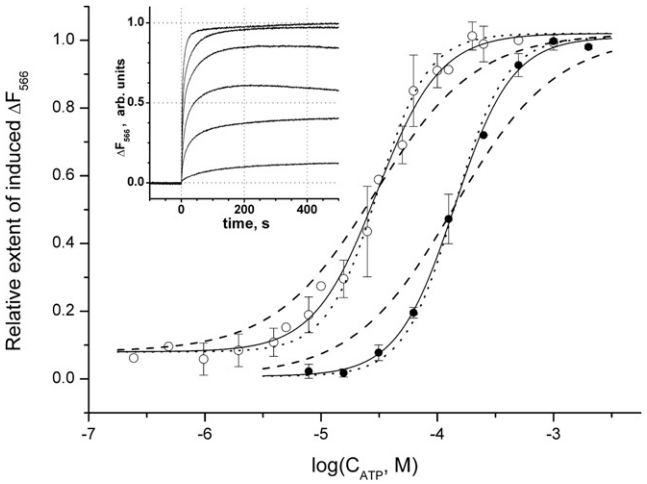

FIGURE 3 ATP titration of subunit ε conformational transition as monitored via fluorescence of Cy3 at 566 nm in F_1 (*open circles*) and F_OF_1 (*solid circles*). Measurements were done at 59°C in buffer containing 100 mM KCl, 1 mM $MgCl_2$, 20 mM MES, 20 mM MOPS, 20 mM HEPES, 20 mM Tricine, 10% v/v glycerol, pH 7.9. The fluorescence change was induced by addition of ATP to the respective final concentration (*x* axis), and the change extent was measured after the plateau was reached (*y* axis, normalized by the fluorescence change extent after addition of ATP to 1 mM). Trace with water added instead of ATP was used as baseline. The inset shows an example of experimental traces in which ATP was added to a WT F_1 sample at time 0 to final concentrations of 1 mM, 250 μM, 62.5 μM, 31.25 μM, 15.6 μM, and 7.8 μM (*top* to *bottom*). Each data point was measured in triplicate or more, and the standard deviation is plotted as error bars. Solid lines represent the best fits of the data points with a Hill function, dotted lines are fits with a Hill number of 2, and dashed lines are fits with a Hill number of 1.

TABLE 1 Kinetic parameters (time constants and relative inputs of components) of subunit ε conformational transitions induced by addition of ATP to 1 mM at 59°C

Sample	τ_1, s	A1, %	τ_2, s	A2, %	*n*
WT F_1	1.3 ± 0.3	58 ± 8	9.6 ± 2.4	42 ± 8	9
WT F_OF_1	7.8 ± 2.6	61 ± 4	57 ± 22	39 ± 4	6
βD390A F_1	1.2 ± 0.4	71 ± 8	8.0 ± 2.9	29 ± 8	7
βD390A F_OF_1	3.0 ± 1.4	64 ± 6	18 ± 4	36 ± 6	4
βAALSAAA F_1	0.6 ± 0.3	84 ± 4	5.7 ± 1.6	16 ± 4	7
βAALSAAA F_OF_1	0.9 ± 0.2	80 ± 2	17 ± 3	20 ± 2	3
εEARA F_OF_1	1.8 ± 0.8	60 ± 2	28 ± 2	40 ± 2	4

Traces were fitted with a biexponential function; *n* is the number of traces analyzed.

Role of the βDELSDED region in the conformational transition of ε

The electrostatic interactions of the negatively charged residues in the βDELSDED region of *Bacillus* PS3 ATP synthase were previously demonstrated to play an important role in the inhibition of ATP hydrolysis by subunit ε (43). In this work, we attempted to clarify their role in the conformational transitions of ε. We analyzed two mutants: one with a single substitution βD390A (first Asp in βDELSDED), and one with a full substitution βAALSAAA. According to the previous study (43), the βD390A mutation only slightly reduced (by 20%) the ATPase activity of the $\alpha_3\beta_3\gamma$-complex, and diminished the inhibitory effect of subunit ε threefold. In the βAALSAAA mutant, the inhibitory effect of ε was reduced ninefold, but the ATPase activity of the $\alpha_3\beta_3\gamma$-complex was sevenfold lower than in the WT.

As can be seen in Fig. 4 *A* and *B*, both mutations resulted in acceleration of the ε transition induced by 1 mM ATP. The effect was clear in both isolated F_1 and the whole F_OF_1. A detailed analysis revealed that the kinetics of transition in the mutants was also apparently biexponential for both isolated F_1 and the whole F_OF_1 (Table 1).

In the βD390A mutant, the slight acceleration observed in isolated F_1 was not due to the change in the time constants of transition kinetic components; rather, it reflected the increase in the fast component relative input (from ≈60% in the WT to ≈70% in the βD390A mutant). In contrast, the same mutation in the whole F_OF_1 led to an ~3-fold decrease in both time constants, leaving the relative inputs unaffected.

In the fully substituted βAALSAAA mutant, the transition time constants for isolated F_1 were ~2-fold smaller than in the WT, and the relative input of the fast component increased from ≈60% to ≈80% (Table 1). The strongest difference was observed in F_OF_1 for the fast component time constant, which dropped more than eightfold (from 7.8 s in the WT to 0.9 s in the βAALSAAA mutant). The slow component was also accelerated (57 s vs. 17 s).

The dependence of the ATP-induced transition extent on ATP concentration in the βD390A and βAALSAAA mutants is shown in Fig. 5. In the case of the βD390A mutant (Fig. 5 *A*), the dependence was very similar to that of the

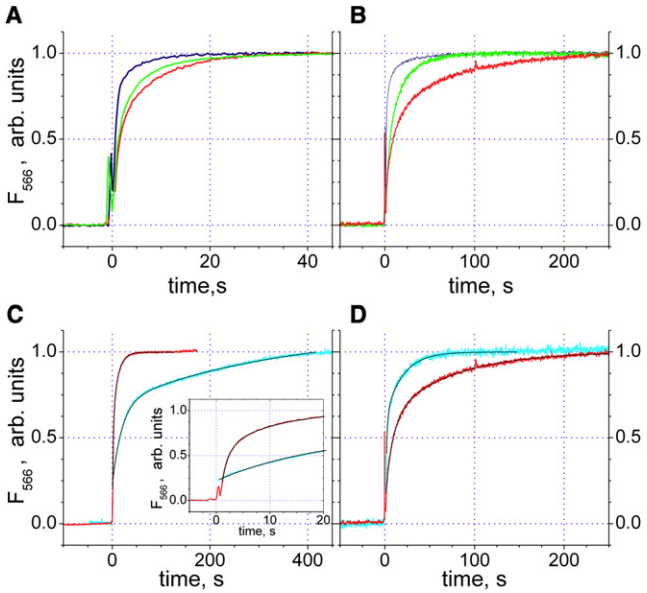

FIGURE 4 Effect of mutations on the kinetics of subunit ε conformational transition induced by 1 mM ATP in F_1 (*A* and *C*) and F_OF_1 (*B* and *D*). Measurements were done at 59°C in buffer containing 100 mM KCl, 1 mM $MgCl_2$, 20 mM MES, 20 mM MOPS, 20 mM HEPES, 20 mM Tricine, 10% v/v glycerol, pH 7.9. (*A* and *B*) βDELSDED mutants (*red trace*: WT; *green trace*: βD390A mutant; *blue trace*: βAALSAAA mutant). (*C* and *D*) εEARA mutant (*red trace*: WT; *cyan trace*: εEARA mutant). The inset in panel *C* shows the same traces during first 20 s after addition of ATP. ATP added at time 0 to a final concentration of 1 mM. Traces were scaled to the same maximal extent. Note the different timescales.

WT (Fig. 3) for both isolated F_1 (*open circles*) and F_OF_1 (*solid circles*). In the case of the βAALSAAA mutant (Fig. 5 *B*), the apparent K_d was markedly lower than in the WT for both the isolated F_1 (5.6 μM vs. 30 μM) and F_OF_1 (15 μM vs. 141 μM). The Hill number in mutant F_OF_1 was also significantly decreased: a value of $n \approx 0.8$ was observed (compared to $n \approx 1.8$ in the WT).

Role of ATP binding directly to subunit ε in its conformational transitions

To investigate the role of ATP binding directly to subunit ε, we substituted two residues involved in this binding (εGlu-83 and εArg-92 (47); *orange spheres* in Fig. 1 *A*) to alanines. The resultant mutant was named εEARA. Isolated subunit ε with this double mutation had very low ATP binding; the apparent K_d was >1 mM at 25°C (F. Kadoya and Y. Kato-Yamada, unpublished observations). Taking into account the fact that the WT showed >100-fold lower ATP binding at 60°C than at 25°C (48), there must have been negligible, if any, ATP binding to the εEARA mutant at 59°C with 1 mM ATP in this study.

The ATPase activity of isolated εEARA F_1 (1 mM ATP, 59°C) was indistinguishable from that of the WT F_1. However, in the whole εEARA F_OF_1 (isolated or incorporated in liposomes), the rate of ATP hydrolysis was 60% ± 7% of the WT rate.

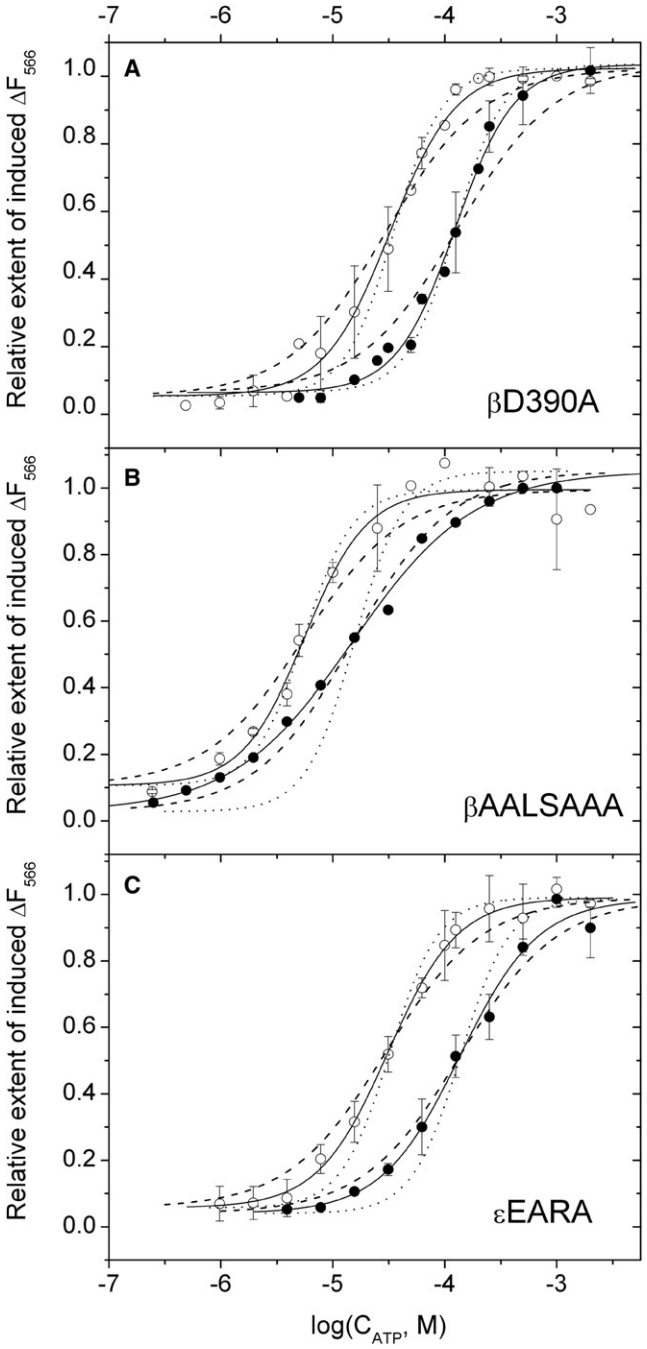

FIGURE 5 ATP titration of subunit ε conformational transition as monitored via fluorescence of Cy3 at 566 nm in F_1 (*open circles*) and F_OF_1 (*solid circles*). Measurements were done as in Fig. 3. Solid lines represent the best fits of the data points with a Hill function, dotted lines are fits with a Hill number of 2, and dashed lines are fits with a Hill number of 1. (*A*) βD390A mutant. (*B*) βAALSAAA mutant. (*C*) εEARA mutant. Standard deviation is plotted as error bars for data points measured in triplicate; other data points are the average of two measurements. Solid lines represent the best fits of the data points with a Hill function, dotted lines are fits with a Hill number of 2, and dashed lines are fits with a Hill number of 1.

A comparison of the ATP-induced conformational change of ε in the WT and in the mutant enzyme is shown in Fig. 4, *C* and *D*. In the isolated F_1, the mutation slowed

TABLE 2 Apparent K_d and Hill number for the dependence of the donor fluorescence change extent on ATP concentration

Sample	Apparent K_d, μM	Hill number
WT F_1	30 ± 2	1.60 ± 0.14
WT F_OF_1	141 ± 8	1.76 ± 0.13
βD390A F_1	30 ± 2	1.60 ± 0.13
βD390A F_OF_1	124 ± 9	1.65 ± 0.17
βAALSAAA F_1	5.6 ± 0.8	1.57 ± 0.33
βAALSAAA F_OF_1	15 ± 2	0.81 ± 0.19
εEARA F_1	31 ± 2	1.39 ± 0.11
εEARA F_OF_1	136 ± 19	1.24 ± 0.24

the transition down. As can be seen in Fig. 4 *C*, the kinetics was no longer biexponential. Immediately after the addition of ATP, a fast, unresolved change in the fluorescence was observed (see the *inset* in Fig. 4 *C*). This fast component accounted for ≈20% of the total fluorescence change. It was followed by a biexponential increase of the signal with time constants of ≈20 s and ≈320 s.

In the whole F_OF_1, the mutation effect was the opposite of that observed in isolated F_1: the conformational transition of ε was faster in εEARA. No unresolved initial phase was observed, and the kinetics could be fitted with a biexponential function (Table 1).

The ATP titration curves for the εEARA mutant are shown in Fig. 5 *C*. The apparent K_d values were very close to these of the WT F_1 (Table 2). The Hill number was somewhat reduced in the mutant, especially in the whole F_OF_1 ($n \approx 1.2$ vs. $n \approx 1.8$ in the WT).

Influence of the subunit ε conformation on the ATPase activity of F_OF_1 in *Bacillus* PS3 membranes

It has been established that the extended conformation of subunit ε is inhibitory and the contracted hairpin conformation is not (42). Moreover, in our previous study on isolated F_1 in the presence of the ATP regenerating system, it was determined that the fast kinetic component of the Cy3 fluorescence change correlated with the increase in the ATPase activity of the enzyme (48). However, we believed that additional experiments in membrane samples at 59°C were necessary.

To investigate the effect of the subunit ε conformation on F_OF_1 ATPase activity, *Bacillus* PS3 membranes stripped of F_1 with EDTA and treated with NBD-Cl to block any residual ATPase activity were reconstituted with four types of F_1: 1), the WT γCy3\$\varepsilon$Cy5-labeled F_1 used throughout this work; 2), the $\varepsilon^{\Delta C}$-F_1 with the C-terminal domain of subunit ε deleted (used as a control with zero inhibitory effect of ε); 3), the unlabeled $\gamma_c\varepsilon_c$-F_1 treated with $CuCl_2$ in the absence of ATP to fix subunit ε in the extended state by a cross-link as described previously (42) (used as a control with a maximal inhibitory effect of ε); and 4), the latter $\gamma_c\varepsilon_c$-F_1 cross-linked enzyme treated with DTT to break the cross-link (used as a control mimicking the WT enzyme).

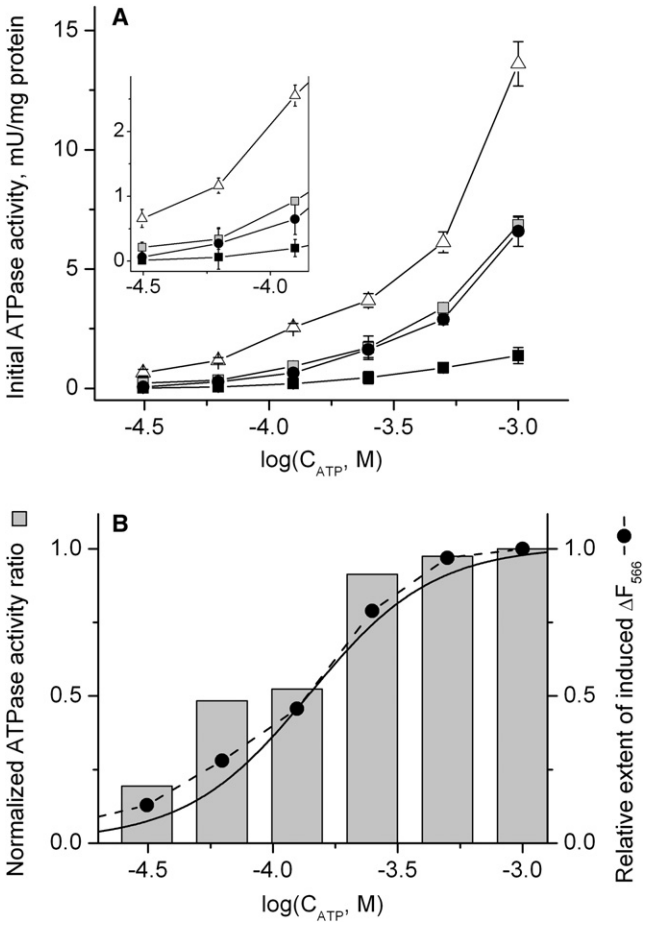

FIGURE 6 ATPase activity of F_OF_1 in *Bacillus* PS3 membranes and its correlation with the Cy3 fluorescence changes. Measurements were done at 59°C. See details in text. (*A*) Dependence of the initial ATPase activity on ATP concentration. *Bacillus* PS3 membranes reconstituted with different F_1 samples were diluted to 9 μg protein/mL with buffer containing 1 mM tricine-KOH (pH 8.05), 150 mM KCl, 1 mM $MgCl_2$, 50 μM phenol red. ATP hydrolysis was started by addition of ATP to the desired final concentration (*x* axis, note the log scale). Open triangles: $\varepsilon^{\Delta C}$ F_OF_1; black circles: γCy3/εCy5 F_OF_1; black squares: $\gamma_c\varepsilon_c$ F_OF_1 with subunit ε fixed in the extended state by a cross-link; gray squares: $\gamma_c\varepsilon_c$ F_OF_1 without cross-link. The inset shows the same data (low ATP concentration part) with higher resolution. Each point was measured at least in triplicate. (*B*) Relative effect of subunit ε C-terminus on ATPase activity at different ATP concentrations. Gray columns: The activity of γCy3/εCy5 F_OF_1 was divided by the activity of $\varepsilon^{\Delta C}$ F_OF_1 and normalized to one at an ATP concentration of 1 mM. Solid circles: ATP titration of subunit ε conformational transition in γCy3/εCy5 F_OF_1 monitored via fluorescence of Cy3 at 566 nm (same conditions as for ATP hydrolysis measurements). Solid line: Hill function best fit of F_OF_1 ATP titration data duplicated from Fig. 3.

After reconstitution with F_1, the initial ATPase activity was measured in each sample at different ATP concentrations (Fig. 6 *A*). In all samples, the ATPase activity decreased when the ATP concentration was lowered. However, this decrease was less pronounced in $\varepsilon^{\Delta C}$-F_OF_1 than in other samples. We normalized the ATPase activity by the value at 1 mM ATP and plotted the ratio of normalized activity in the γCy3\$\varepsilon$Cy5-labeled F_OF_1 to normalized activity in

the $\varepsilon^{\Delta C}$ sample. The relative decrease in ATPase activity at lower ATP concentrations was more than twofold larger in γCy3\εCy5-labeled F_OF_1 than in $\varepsilon^{\Delta C}$-F_OF_1 (Fig. 6 *B*, *gray columns*). To directly compare this effect with the ATP-induced FRET change, we also measured the FRET change in γCy3\εCy5-labeled F_OF_1 sample in the same buffer that was used for ATPase activity measurements (Fig. 6 *B*, *solid circles*). The results indicated a good correlation between the relative FRET change and the relative ATPase activity.

DISCUSSION

We extended the FRET technique that was successfully applied for real-time monitoring of subunit ε conformational transitions in isolated F_1 to the whole F_OF_1 integrated in *Bacillus* PS3 inverted membrane vesicles. The enzyme was studied in a native lipid environment at 59°C (close to 65°C, the optimal growth temperature for *Bacillus* PS3). No ATP regenerating system or glucose\hexokinase trap was added during the measurements, so both ATP and ADP were present in the medium, as they would be in vivo. Unfortunately, the reconstituted membranes were not well coupled at 59°C (see the Supporting Material). Therefore, the results describe F_OF_1 incorporated into uncoupled membrane with no significant proton-motive force present.

The results shown in Fig. 2 indicate that in the absence of ATP, subunit ε was in the extended state (highest FRET efficiency, lowest Cy3 fluorescence), irrespective of the presence of ADP. ATP induced the transition of ε to a contracted state, again irrespective of the presence of ADP (although ADP slowed the transition down ~5-fold; Fig. 2 *B*). Moreover, the addition of ADP in fourfold excess did not reverse the ATP-induced transition. These findings suggest that the equilibrium between the contracted and extended conformations of ε was influenced only by the ATP concentration, and not by ATP/ADP ratio.

The ATP titration of the subunit ε conformational transition (Fig. 3) revealed that the apparent K_d for transition is 141 μM. ATP titration of the ATPase activity in the γCy3\εCy5-labeled F_OF_1 used for FRET measurements, and in $\varepsilon^{\Delta C}$-F_OF_1 that lacked the inhibitory C-terminal domain of ε (Fig. 6) indicated that the observed conformational transition correlated well with the increase in the subunit ε inhibitory effect. Unless some unknown factors significantly alter the behavior of subunit ε in vivo, these results imply that the hairpin noninhibitory conformation of ε prevails under normal physiological conditions (when intracellular ATP concentration is in the millimolar range). In contrast, the extended inhibitory state of ε is expected to occur only when the intracellular ATP concentration decreases to $\leq$100–200 μM. It is tempting to speculate that in *Bacillus* PS3 ATP synthase, subunit ε serves as an ''emergency break'' that strongly inhibits the ATP hydrolysis activity of the enzyme when the intracellular ATP pool is almost exhausted. Further experiments are necessary to prove or dismiss this hypothesis.

A Hill number higher than one (Fig. 3 and Table 2) indicated that binding of at least two ATP molecules per enzyme was necessary to induce the transition of ε. A noninteger Hill number suggested that the mechanism of transition induction was complex and could not be described in the framework of a simple two-site cooperative binding model. From a physiological point of view, a higher Hill number results in a narrower interval of ATP concentrations where the transition occurs, i.e., an increase in the Hill number shifts the response of the system from a gradual to an ''all-or-nothing'' reaction triggered by a decrease/increase of ATP concentration below/above a certain limit.

The list of known nucleotide-binding sites on F_OF_1 includes three catalytic sites and three noncatalytic sites on the $\alpha_3\beta_3$ hexamer, and one site on subunit ε . However, we note that 1), in isolated F_1 the deletion of the noncatalytic sites did not abolish the ATP-induced transitions of subunit ε (34,48); 2), as can be seen in Figs. 4 and 5, the deletion of the nucleotide-binding site on subunit ε did not abolish these transitions either; and 3), previous studies revealed that in isolated F_1 the deletion of the catalytic sites resulted in the loss of an ATP-induced conformational change of subunit ε, as detected by cross-linking (47). Therefore, it is likely that MgATP binding to the catalytic sites is the primary event that induces the conformational transition of subunit ε, as was proposed previously (48).

Taking into consideration that the apparent K_d value was 141 μM for the ε transition (Table 2), it is probable that all three catalytic sites have to be occupied to drive the subunit ε transition from the inhibitory extended state. It should be noted that in the βAALSAAA mutant F_OF_1, the apparent K_d value was lower than that of the WT by one order of magnitude, and there was no indication of positive cooperativity in ATP binding (Hill number < 1; see Fig. 5 *B*, *solid circles*, and Table 2). Probably in this case, binding of ATP to one catalytic site (or two) was sufficient to induce the transition of ε.

The apparent K_d value of 15 μM for the βAALSAAA mutant from the ATP titration experiment (Table 2) suggests that interactions of acid residues in βDELSDED are involved in stabilizing the extended conformation of subunit ε, as was hypothesized in an earlier study (52). It should be noted that the first Asp in βDELSDED does not seem to be involved in such interactions, because its replacement to Ala had no detectable effect on the ATP titration curve in either F_OF_1 or isolated F_1 (Table 2). However, this replacement diminishes the inhibitory effect of ε by a factor of 3 (43). Our results also indicate that this replacement accelerated the ATP-induced transition of subunit ε (Table 1). It is therefore likely that the interactions between the first Asp in βDELSDED and the C-terminus of ε occurred in some intermediate, transitional state that differed from the stable, fully extended conformation, although they were also inhibitory.

The kinetics of the ATP-induced conformational change of subunit ε was apparently biexponential in both F_1 and F_OF_1 (Table 1 and Fig. S2). Such kinetics could be expected if the transition of the ε C-terminus were a complex process with two or more stages. Therefore, it is probable that there are some intermediate conformation(s) between the fully extended state, in which the C-terminus of ε is in close proximity to the N-terminus of γ, and a fully contracted hairpin-like state. Of note, the relative inputs of the fast and slow kinetic components were the same for isolated F_1 and F_OF_1 (Table 1). Therefore, it seems likely that the conformational transition of subunit ε follows the same pattern and has the same intermediate state(s) in isolated F_1 and whole F_OF_1.

In this work, we were also interested in clarifying the role of ATP binding to ε. A previous study revealed that alanine replacements of residues involved in ATP binding to ε enhanced the inhibitory effect (47). In agreement with these results, ATPase activity in εEARA mutant F_OF_1 was also diminished (60% of the WT activity). This was in apparent contradiction to the results documented in Figs. 4 and 5. On the one hand, we observed that in the εEARA mutant, ATP induced a conformational transition of ε similar to that in the WT enzyme. Therefore, one could expect full inhibition relief at millimolar ATP concentrations. On the other hand, in εEARA F_OF_1, a 40% inhibition of the steady-state ATP hydrolysis was observed at 1 mM ATP (i.e., at this ATP concentration, the mutant subunit ε was no longer in the extended state, but was still inhibitory). Our results suggest that the transition of ε from the extended state to some contracted state was necessary but was not sufficient to eliminate the inhibition of ATPase activity. A specific hairpin-like fold stabilized by bound ATP was probably essential for full activity. Unlike subunit ε from *E. coli* F_OF_1, *Bacillus* PS3 subunit ε requires ATP binding to keep its C-terminus in a hairpin fold (46). Thus, in the εEARA mutant, the subunit ε C-terminus probably remained unfolded and inhibitory even at high ATP concentrations (state *II* in Fig. 1 *B*). Such behavior is indistinguishable from the transition to the hairpin conformation (state *III* in Fig. 1 *B*) revealed by the FRET measurements, because in both cases the distance from Cy5 at the C-terminus of ε to Cy3 at the N-terminus of subunit γ significantly increased.

Our results and earlier data can be explained by the following simple scheme (Fig. 1 *B*): At low ATP concentrations, ε is in the inhibitory extended state (state *I*). Binding of the MgATP complex to the catalytic sites induces conformational changes that drive the C-terminal domain of ε out of the $\alpha_3\beta_3$ hexamer (Fig. 1 *B*, *I*→*II*). In the hypothetical intermediate state (state *II*), the C-terminus of ε may be able to adopt different conformations, some of which could be inhibitory of ATPase activity (as was observed in εEARA F_OF_1). Other, noninhibitory conformations include the contracted hairpin state. In the WT enzyme (but not in the εEARA mutant), the noninhibitory hairpin state is stabilized by binding of ATP (Fig. 1 *B*, *II*→*III*). If the ATP concentration later drops below the apparent K_d of ATP binding to ε ($\approx$200 μM at 59°C (48)), ATP will dissociate from subunit ε, thereby destabilizing the hairpin fold (Fig. 1 *B*, *III*→*II*). A further decrease in ATP concentration below the apparent K_d of the ε conformational transition (141 μM at 59°C; see Table 2) leads to a reverse transition of subunit ε (Fig. 1 *B*, *II*→*I*) and a strong inhibition of ATP hydrolysis.

SUPPORTING MATERIAL

Additional materials and methods, results and discussion, six figures, and references are available at http://www.biophysj.org/biophysj/supplemental/S0006-3495(09)01630-0.

The authors thank Prof. Toru Hisabori, Prof. Stanley Dunn, Dr. Ryota Iino, Dr. Hiroki Konno, and Eiichiro Saita for fruitful and stimulating discussions, and Chiaki Wakabayashi for excellent technical assistance.

REFERENCES

1. von Ballmoos, C., G. M. Cook, and P. Dimroth. 2008. Unique rotary ATP synthase and its biological diversity. *Annu. Rev. Biophys.* 37:43–64.
2. Feniouk, B. A., and M. Yoshida. 2008. Regulatory mechanisms of proton-translocating FOF1-ATP synthase. *In* Bioenergetics. G. Schaefer and H. S. Penefsky, editors. Springer, Berlin/Heidelberg. 279–308.
3. Abrahams, J. P., A. G. Leslie, …, J. E. Walker. 1994. Structure at 2.8 A resolution of F_1-ATPase from bovine heart mitochondria. *Nature.* 370:621–628.
4. Hausrath, A. C., G. Grüber, …, R. A. Capaldi. 1999. Structural features of the γ subunit of the *Escherichia coli* F(1) ATPase revealed by a 4.4-A resolution map obtained by x-ray crystallography. *Proc. Natl. Acad. Sci. USA.* 96:13697–13702.
5. Groth, G., and E. Pohl. 2001. The structure of the chloroplast F_1-ATPase at 3.2 A resolution. *J. Biol. Chem.* 276:1345–1352.
6. Stock, D., A. G. Leslie, and J. E. Walker. 1999. Molecular architecture of the rotary motor in ATP synthase. *Science.* 286:1700–1705.
7. Seelert, H., A. Poetsch, …, D. J. Müller. 2000. Structural biology. Proton-powered turbine of a plant motor. *Nature.* 405:418–419.
8. Stahlberg, H., D. J. Müller, …, P. Dimroth. 2001. Bacterial $Na(^+)$-ATP synthase has an undecameric rotor. *EMBO Rep.* 2:229–233.
9. Pogoryelov, D., Y. Nikolaev, …, T. Meier. 2008. Probing the rotor subunit interface of the ATP synthase from *Ilyobacter tartaricus*. *FEBS J.* 275:4850–4862.
10. Noji, H., R. Yasuda, …, K. Kinosita, Jr. 1997. Direct observation of the rotation of F_1-ATPase. *Nature.* 386:299–302.
11. Junge, W., O. Pänke, …, S. Engelbrecht. 2001. Inter-subunit rotation and elastic power transmission in F_0F_1-ATPase. *FEBS Lett.* 504: 152–160.
12. Diez, M., B. Zimmermann, …, P. Gräber. 2004. Proton-powered subunit rotation in single membrane-bound F_0F_1-ATP synthase. *Nat. Struct. Mol. Biol.* 11:135–141.
13. Rondelez, Y., G. Tresset, …, H. Noji. 2005. Highly coupled ATP synthesis by F_1-ATPase single molecules. *Nature.* 433:773–777.
14. Junge, W., H. Sielaff, and S. Engelbrecht. 2009. Torque generation and elastic power transmission in the rotary F(O)F(1)-ATPase. *Nature.* 459:364–370.
15. Nakamoto, R. K., J. A. Baylis Scanlon, and M. K. Al-Shawi. 2008. The rotary mechanism of the ATP synthase. *Arch. Biochem. Biophys.* 476:43–50.
16. Ariga, T., E. Muneyuki, and M. Yoshida. 2007. F_1-ATPase rotates by an asymmetric, sequential mechanism using all three catalytic subunits. *Nat. Struct. Mol. Biol.* 14:841–846.

17. Capaldi, R. A., and R. Aggeler. 2002. Mechanism of the F(1)F(0)-type ATP synthase, a biological rotary motor. *Trends Biochem. Sci.* 27: 154–160.

18. Capaldi, R. A., and B. Schulenberg. 2000. The ε subunit of bacterial and chloroplast F(1)F(0) ATPases. Structure, arrangement, and role of the ε subunit in energy coupling within the complex. *Biochim. Biophys. Acta.* 1458:263–269.

19. Vik, S. B. 2000. What is the role of ε in the *Escherichia coli* ATP synthase? *J. Bioenerg. Biomembr.* 32:485–491.

20. Feniouk, B. A., T. Suzuki, and M. Yoshida. 2006. The role of subunit ε in the catalysis and regulation of F_OF_1-ATP synthase. *Biochim. Biophys. Acta.* 1757:326–338.

21. Kuki, M., T. Noumi, …, M. Futai. 1988. Functional domains of ε subunit of *Escherichia coli* H+-ATPase (F0F1). *J. Biol. Chem.* 263:17437–17442.

22. Cruz, J. A., B. Harfe, …, R. E. McCarty. 1995. Molecular dissection of the ε subunit of the chloroplast ATP synthase of spinach. *Plant Physiol.* 109:1379–1388.

23. Xiong, H., D. Zhang, and S. B. Vik. 1998. Subunit ε of the *Escherichia coli* ATP synthase: novel insights into structure and function by analysis of thirteen mutant forms. *Biochemistry.* 37:16423–16429.

24. Kato-Yamada, Y., D. Bald, …, M. Yoshida. 1999. ε Subunit, an endogenous inhibitor of bacterial F(1)-ATPase, also inhibits F(0)F(1)-ATPase. *J. Biol. Chem.* 274:33991–33994.

25. Nowak, K. F., and R. E. McCarty. 2004. Regulatory role of the C-terminus of the ε subunit from the chloroplast ATP synthase. *Biochemistry.* 43:3273–3279.

26. Cipriano, D. J., and S. D. Dunn. 2006. The role of the ε subunit in the *Escherichia coli* ATP synthase. The C-terminal domain is required for efficient energy coupling. *J. Biol. Chem.* 281:501–507.

27. Keis, S., A. Stocker, …, G. M. Cook. 2006. Inhibition of ATP hydrolysis by thermoalkaliphilic F_1F_0-ATP synthase is controlled by the C-terminus of the ε subunit. *J. Bacteriol.* 188:3796–3804.

28. Iino, R., R. Hasegawa, …, H. Noji. 2009. Mechanism of inhibition by C-terminal α-helices of the ε subunit of *Escherichia coli* FoF1-ATP synthase. *J. Biol. Chem.* 284:17457–17464.

29. Richter, M. L., and R. E. McCarty. 1987. Energy-dependent changes in the conformation of the ε subunit of the chloroplast ATP synthase. *J. Biol. Chem.* 262:15037–15040.

30. Mendel-Hartvig, J., and R. A. Capaldi. 1991. Nucleotide-dependent and dicyclohexylcarbodiimide-sensitive conformational changes in the ε subunit of *Escherichia coli* ATP synthase. *Biochemistry.* 30:10987–10991.

31. Dallmann, H. G., T. G. Flynn, and S. D. Dunn. 1992. Determination of the 1-ethyl-3-[(3-dimethylamino)propyl]-carbodiimide-induced cross-link between the β and ε subunits of *Escherichia coli* F1-ATPase. *J. Biol. Chem.* 267:18953–18960.

32. Aggeler, R., and R. A. Capaldi. 1996. Nucleotide-dependent movement of the ε subunit between α and β subunits in the *Escherichia coli* F1F0-type ATPase. *J. Biol. Chem.* 271:13888–13891.

33. Wilkens, S., and R. A. Capaldi. 1998. Solution structure of the ε subunit of the F1-ATPase from *Escherichia coli* and interactions of this subunit with β subunits in the complex. *J. Biol. Chem.* 273:26645–26651.

34. Kato-Yamada, Y., M. Yoshida, and T. Hisabori. 2000. Movement of the helical domain of the ε subunit is required for the activation of thermophilic F_1-ATPase. *J. Biol. Chem.* 275:35746–35750.

35. Zimmermann, B., M. Diez, …, M. Börsch. 2005. Movements of the ε-subunit during catalysis and activation in single membrane-bound $H(^+)$-ATP synthase. *EMBO J.* 24:2053–2063.

36. Uhlin, U., G. B. Cox, and J. M. Guss. 1997. Crystal structure of the ε subunit of the proton-translocating ATP synthase from *Escherichia coli*. *Structure.* 5:1219–1230.

37. Wilkens, S., F. W. Dahlquist, …, R. A. Capaldi. 1995. Structural features of the ε subunit of the *Escherichia coli* ATP synthase determined by NMR spectroscopy. *Nat. Struct. Biol.* 2:961–967.

38. Gibbons, C., M. G. Montgomery, …, J. E. Walker. 2000. The structure of the central stalk in bovine F(1)-ATPase at 2.4 A resolution. *Nat. Struct. Biol.* 7:1055–1061.

39. Rodgers, A. J. W., and M. C. J. Wilce. 2000. Structure of the γ-ε complex of ATP synthase. *Nat. Struct. Biol.* 7:1051–1054.

40. Hausrath, A. C., R. A. Capaldi, and B. W. Matthews. 2001. The conformation of the ε- and γ-subunits within the *Escherichia coli* F(1) ATPase. *J. Biol. Chem.* 276:47227–47232.

41. Tsunoda, S. P., A. J. Rodgers, …, R. A. Capaldi. 2001. Large conformational changes of the ε subunit in the bacterial F_1F_0 ATP synthase provide a ratchet action to regulate this rotary motor enzyme. *Proc. Natl. Acad. Sci. USA.* 98:6560–6564.

42. Suzuki, T., T. Murakami, …, M. Yoshida. 2003. F_0F_1-ATPase/synthase is geared to the synthesis mode by conformational rearrangement of ε subunit in response to proton motive force and ADP/ATP balance. *J. Biol. Chem.* 278:46840–46846.

43. Hara, K. Y., Y. Kato-Yamada, …, M. Yoshida. 2001. The role of the βDELSEED motif of F1-ATPase: propagation of the inhibitory effect of the ε subunit. *J. Biol. Chem.* 276:23969–23973.

44. Kato-Yamada, Y., and M. Yoshida. 2003. Isolated ε subunit of thermophilic F_1-ATPase binds ATP. *J. Biol. Chem.* 278:36013–36016.

45. Iizuka, S., S. Kato, …, Y. Kato-Yamada. 2006. $\gamma\varepsilon$ Sub-complex of thermophilic ATP synthase has the ability to bind ATP. *Biochem. Biophys. Res. Commun.* 349:1368–1371.

46. Yagi, H., N. Kajiwara, …, H. Akutsu. 2007. Structures of the thermophilic F_1-ATPase ε subunit suggesting ATP-regulated arm motion of its C-terminal domain in F_1. *Proc. Natl. Acad. Sci. USA.* 104:11233–11238.

47. Kato, S., M. Yoshida, and Y. Kato-Yamada. 2007. Role of the ε subunit of thermophilic F_1-ATPase as a sensor for ATP. *J. Biol. Chem.* 282:37618–37623.

48. Iino, R., T. Murakami, …, M. Yoshida. 2005. Real-time monitoring of conformational dynamics of the ε subunit in F_1-ATPase. *J. Biol. Chem.* 280:40130–40134.

49. Suzuki, T., H. Ueno, …, M. Yoshida. 2002. F(0) of ATP synthase is a rotary proton channel. Obligatory coupling of proton translocation with rotation of *c*-subunit ring. *J. Biol. Chem.* 277:13281–13285.

50. Ahmad, Z., and A. E. Senior. 2005. Modulation of charge in the phosphate binding site of *Escherichia coli* ATP synthase. *J. Biol. Chem.* 280:27981–27989.

51. Feniouk, B. A., T. Suzuki, and M. Yoshida. 2007. Regulatory interplay between proton motive force, ADP, phosphate, and subunit ε in bacterial ATP synthase. *J. Biol. Chem.* 282:764–772.

52. Feniouk, B. A., and W. Junge. 2005. Regulation of the F_0F_1-ATP synthase: the conformation of subunit ε might be determined by directionality of subunit γ rotation. *FEBS Lett.* 579:5114–5118.

53. Humphrey, W., A. Dalke, and K. Schulten. 1996. VMD: visual molecular dynamics. *J. Mol. Graph.* 14:33–38, 27–28.